Title

Electrical generation and methane emission from an anoxic riverine sediment slurry treated by a two-chamber microbial fuel cell

Journal

Environmental Science and Pollution Research, 29(31)

ISSN

0944-1344

Authors

Xiao, Jiahui
Yang, Yue
Hu, Fengjie
et al.

Publication Date

2022-07-01

DOI

10.1007/s11356-022-19292-x

Peer reviewed

Environmental Science and Pollution Research
https://doi.org/10.1007/s11356-022-19292-x

RESEARCH ARTICLE

Electrical generation and methane emission from an anoxic riverine sediment slurry treated by a two-chamber microbial fuel cell

Jiahui Xiao[1] · Yue Yang[1] · Fengjie Hu[1] · Taiping Zhang[1] · Randy A. Dahlgren[2]

Received: 8 November 2021 / Accepted: 14 February 2022

Abstract

A two-chamber slurry microbial fuel cell (SMFC) was constructed using black-odorous river sediments as substrate for the anode. We tested addition of potassium ferricyanide ($K_3[Fe(CN)_6]$) or sodium chloride (NaCl) to the cathode chamber (0, 50, 100, 150, and 200 mM) and aeration of the cathode chamber (0, 2, 4, 6, and 8 h per day) to assess their response on electrical generation, internal resistance, and methane emission over a 600-h period. When the aeration time in the cathode chamber was 6 h and $K_3[Fe(CN)_6]$ or NaCl concentrations were 200 mM, the highest power densities were 6.00, 6.45, and 6.64 mW·m^{-2}, respectively. With increasing $K_3[Fe(CN)_6]$ or NaCl concentration in the cathode chamber, methane emission progressively decreased (mean ± SD: 181.6 ± 10.9 → 75.5 ± 9.8 mg/m^3·h and 428.0 ± 28.5 → 157.0 ± 35.7 mg/m^3·h), respectively, but was higher than the reference having no cathode/anode electrodes (~ 30 mg/m^3·h). Cathode aeration (0 → 8 h/day) demonstrated a reduction in methane emission from the anode chamber for only the 6-h treatment (mean: 349.6 ± 37.4 versus 299.4 ± 34.7 mg/m^3·h for 6 h/day treatment); methane emission from the reference was much lower (85.3 ± 26.1 mg/m^3·h). Our results demonstrate that adding an electron acceptor ($K_3[Fe(CN)_6]$), electrolyte solution (NaCl), and aeration to the cathode chamber can appreciably improve electrical generation efficiency from the MFC. Notably, electrical generation stimulates methane emission, but methane emission decreases at higher power densities.

Keywords Microbial fuel cell · Electricity generation · Power density · Methane emission · Pollution remediation

Introduction

Microbial fuel cells (MFC) refer to a technology that transfers chemical energy to electrical energy, as facilitated by microbial decomposition of organic matter. These microbes, termed electricigens, create the possibility of converting organic compounds into electricity in self-sustaining systems (Greenman et al. 2019; Lovley 2006). Mechanistically, microbes decompose organic matter in the anode chamber under anaerobic conditions generating electrons, as well as protons. The electrons released in the anode compartment are transferred to the cathode, thereby generating an electrical current through an external circuit. Concomitantly, the protons are transferred to the cathode through a proton exchange membrane where they react with an oxidizer (usually O_2) to form water (Almatouq et al. 2020; Catal et al. 2008). Sediment or slurry microbial fuel cells (SMFCs) are an adaptation of reactor-type MFCs, where the anode and cathode are contained in one- or two-closed compartments. SMFCs typically consist of an anode electrode embedded in the anaerobic sediment and a cathode electrode suspended in

Responsible Editor: Weiming Zhang.

Highlights

1. The presence of electrodes stimulated microbial activity and methane emission.
2. As the concentration of electron acceptor ($K_3[Fe(CN)_6]$) and electrolyte (NaCl) increased from 0 to 200 mM, the power density can be increased (4.50 → 6.45 mW·m^{-2} and 4.47 → 6.64 mW·m^{-2}).
3. When the aeration time in the cathode chamber was 6 h and $K_3[Fe(CN)_6]$ or NaCl concentrations were 200 mM, the power density reached the highest (6.00, 6.45, and 6.64 mW·m^{-2}, respectively), methane emission was the lowest (299.4 ± 34.7, 75.5 ± 9.8, and 157.0 ± 35.7 mg/m^3·h), and total gas production was the highest (82, 81, and 78 mL).

✉ Taiping Zhang
lckzhang@scut.edu.cn

[1] College of Environment and Energy, South China University of Technology, Guangzhou 510006, Guangdong, People's Republic of China

[2] Department of Land, Air and Water Resources, University of California, Davis, CA 95616, USA

the aerobic water column above the anode electrode (Bond 2002; Ewing et al. 2014; Wang et al. 2018).

MFC technology often utilizes miscellaneous organic fuel sources, such as glucose, phenol (Shen et al. 2020), cattle manure slurry (Inoue et al. 2013), algae biomass (Xu et al. 2015), and other environmental organic wastes. Beneficially, electrical energy is generated as chemical energy contained in the organic waste/pollutant is degraded/transformed by microbial processing (Hong et al. 2009; Verma et al. 2021). This provides a remediation strategy in which organic pollutants are degraded along with an overall reduction in the sediment oxygen demand and nutrients. Furthermore, the electrical production of the electrodes affect the mobility and transformation of several redox-sensitive metals (e.g., As, Cr, and Cu) in the sediment, which contribute to their immobilization (Abbas et al. 2017). Thus, SMFCs have the potential as a multi-purpose technology for generating electricity, removing/transforming organic contaminants, reducing sediment oxygen demand and nutrients, and concentrating/immobilizing several heavy metals (Wang &Ren 2014, Zhu et al. 2019).

Several novel SMFCs have been developed for bioelectricity generation and pollutant removal from sediments, such as microalgae-assisted MFC (MA-MFC) (Elshobary et al. 2021), plant microbial fuel cells (PMFC) (Kabutey et al. 2019a, b), and submerged macrophyte sediment microbial fuel cells (SP-SMFC) (Xu et al. 2021a, b). These MFCs have been applied in polluted freshwater environments, wastewater treatment, polluted sediment, and surface water remediation, greenhouse gas mitigation, and biosensing (Hong et al. 2010; Xie et al. 2017). SMFCs have been used to remove pollutants from rivers, lakes, and oceans, as well as artificially flooded environments such as paddy soil, natural wetlands, constructed wetlands, and waste-activated sludge materials (Yang &Chen 2021). For example, black-odorous sediment (i.e., originating from volatile reduced sulfur compounds) remediation by a SMFC resulted in maximum reduction rates for organic matter, total-P, ammonium, and nitrate of 7.8, 30.0, 41.6, and 71.5%, respectively (Yang et al. 2015). Additionally, MFCs were applied as a novel mitigation strategy to attenuate methane (CH_4) emission from paddy fields resulting in reduced methane emission from rice paddies when amended with 0.5% straw (Zhong et al. 2017). Notably, the mechanism(s) and efficiency of MFCs for reducing methane emission have received little research and therefore remain poorly understood (Zhong et al. 2017).

At present, the efficiency of electricity generation by MFCs is low, which limits their economic and practical use for environmental applications. There are a myriad of factors that affect the electrical generation performance of MFCs necessitating the need for further mechanistic-based research to advance their application for environmental remediation. Specifically, the relationship between electrical generation efficiency/performance and methane production is critically needed to advance the practical utilization of MFCs in real-world environments. For example, the electrical generation performance of MFCs can be improved by improving cathode/anode characteristics, such as by treating the anode with inorganic or organic charge transfer mediators (Lowy et al. 2006), or treating the cathode with a nano-composite catalyst (Kodali et al. 2018), low-cost microalgae derived activated biochar (Chakraborty et al. 2020), or manganese oxides (Tatinclaux et al. 2018). Further optimization can be achieved by altering the surface area or area ratio of the cathode and anode (Erbay et al. 2015; Rosenbaum et al. 2006), changing the distance between cathode and anode (Ahn et al. 2014; Rosenbaum et al. 2007), and modifying the substrates in the cathode and anode chambers (Logan et al. 2007). Among these factors, the cathodic electron acceptor has been found to be crucial to MFC performance. The traditional MFCs use dissolved oxygen as cathodic electron acceptor, but nowadays, compared with dissolved oxygen, redox mediators such as ferricyanide (Wei et al. 2012), sodium bromate (Dai et al. 2016), potassium dichromate (Sindhuja et al. 2018), or potassium permanganate (Wang et al. 2019; You et al. 2006), as cathode electron acceptors of MFCs could improve the electricity production of MFCs. Most studies have shown that ferricyanide was excellent cathodic electron acceptor, and MFCs with potassium ferricyanide could avoid oxygen intrusion into the anolyte in comparison to those containing oxygen (Cai et al. 2016), which could maintain anaerobic conditions (Logan et al. 2019), and some exoelectrogenic microorganisms were strict anaerobes in the anodic chamber (Yilmazel et al. 2018), so that ferricyanide could generate relatively a much higher power density than oxygen. Although the standard redox potential of ferricyanide ($E^0 = 0.36$ V) was not as high as that of oxygen ($E^0 = 1.23$ V), it has much lower overpotential, which resulted in not only a faster reaction rate but also much higher power output (Ucar et al. 2017). In addition to this, electrolyte salt concentrations (correlated with ionic strength) have also been shown to affect MFC power output (Rousseau et al. 2013). Miyahara et al. (2015) showed that power output increased as the NaCl concentration increased to 0.1 M, while it was markedly diminished over 0.3 M, and *Geobacteraceae* (electricigens) were not substantially detected in MFCs with NaCl concentrations of 0.3 M or higher (Miyahara et al. 2015). Hence, the optimum salt concentration in MFC was determined by the balance of two factors, namely the solution conductivity and salt tolerance of exoelectrogens. We have previously done studies on electricity generation, sediment remediation, and the diversity of bacterial and archaea communities of SMFCs as a background to our research (Yang et al. 2015; Zhu et al. 2016). Informed by previous studies and following the principles of SMFCs, we constructed two-chambered SMFCs, which

were filled with a sediment slurry in the anode chamber and treated with different electrolyte (potassium ferricyanide and sodium chloride: 0 → 200 mM) and aeration regimes in the cathode chamber. We investigated electrical generation performance and methane emission by the SMFCs under these contrasting experimental treatments, as well as their possible correlations, in order to elucidate operational mechanisms and optimize conditions for application to real-world environments.

Materials and methods

MFC construction

A two-chamber, sediment slurry MFC (SMFC) was constructed using a Perspex cylinder (polymethyl methacrylate) with an effective volume of 500 mL and 10 cm diameter × 10 cm height (Fig. 1). The two compartments were connected with a tube separated by a proton exchange membrane (Grion 0011, Hangzhou Lvhe Environmental Protection Technology Co., LTD, China). Both electrodes consisted of pretreated, activated-carbon fiber felts (Nantong Berg, China) with dimensions of 8 cm × 5 cm × 2 mm. The carbon fiber pretreatment/cleaning procedure followed (Zhu et al. 2011) (i) soaking in acetone for 3 h to remove any oily residues and enhance the hydrophilic nature and biological adsorption of the carbon fiber surface, (ii) rinsing 3–5 times with deionized water, (iii) boiling in deionized water for a total of 3 h with a water change every 0.5 h, (iv) soaking in concentrated sulfuric acid for 5 h and washing with deionized water to a neutral pH, and (v) drying at 20 ℃ in an oven. The treated carbon fiber material was hermetically sealed in a polyethylene bag and stored for subsequent use.

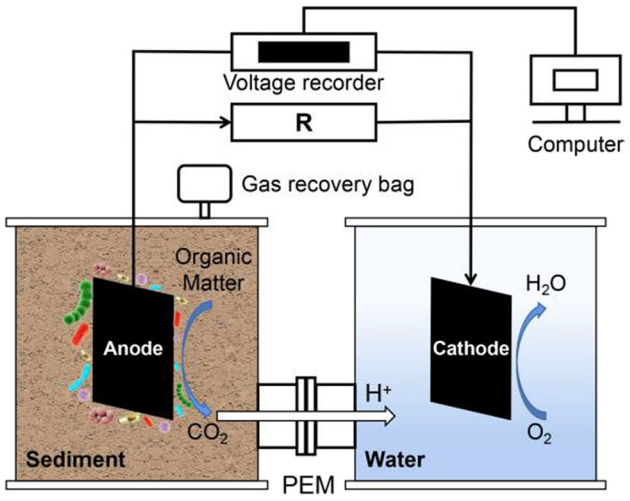

Fig. 1 Diagrammatic drawing of the two-chamber MFC reactor

Electrode poles were placed in the two electrode chambers and connected to the anode or cathode. The anode was fully buried in a sediment slurry and the cathode immersed in an electrolyte solution. The two electrodes were connected with titanium wire to external resistors (1000 Ω) using alligator clips to close the circuit. An identical system was prepared without the electrode connection to serve as a reference state. The sealed anode compartment contained a gas sampling port connected to an evacuated sampling bag to collect gases generated by the system (Zhang et al. 2016). The cathode chamber was open to the atmosphere during operation of the system.

We collected a sediment slurry with a silt loam texture (gray to black colors) from a black-odorous, urban tributary of the Pearl River in Guangzhou, China (23° 07′ 19.99″ N, 113° 23′ 53.28″ E) and used it as a substrate in the anode chamber. Black-odorous sediments form in O_2-depleted sediments when metals precipitate with sulfide and stain the water black; the odorous compounds result from volatile organic and inorganic compounds generated from microbial sulfate reduction or degradation of sulfur-containing organic matter (Liang et al. 2017). At the time of collection, the sediments showed a near-neutral pH (6.86–6.95) and an oxidation–reduction potential of 77–84 mV in the upper sediment layer (0–5 cm). The field sample was homogenized and passed through a 2-mm screen to remove sundries, such as rocks, plastics, and large organic debris. Samples were stored in a sealed/dark PVC bucket and settled for 24 h before the experiments. Since the black-odorous sediment itself contained a large number of microorganisms, it was directly used as a microbial source (natural-mixed bacteria) to start the MFC without any additional pre-culture supplements. Selected physical and chemical characteristics of the sediment slurry were determined by standard methods (Table 1; National Environmental Protection Standard Methods — People's Republic of China).

Startup conditioning of the SMFCs

The startup and operation of the MFC employed a sequential batch culture method. We followed an initial startup procedure for the SMFCs before collecting experimental data that consisted of a batch culture method (Zhu et al. 2019), 500 ml mixed liquid (sediment slurry and nutrient liquid with a volume ratio of 3:2) was inoculated in the MFC anode chamber.

Table 1 Selected physical and chemical properties of sediment slurry used in anode chamber (mean ± std dev; $n = 3$ analytical replicates)

Moisture content (%)	Organic matter (g/kg)	Ammonia-N (mg/kg)	Nitrate–N (mg/kg)	Total phosphorus (mg/kg)
65.7 ± 0.4	65.9 ± 1.3	1.9 ± 0.9	3.7 ± 0.8	899 ± 12

The nutrient solution was a 1 $g \cdot L^{-1}$ glucose nutrient solution, with the following composition: 982.5 mL 50 mM phosphate buffered saline (PBS; 4.576 $g \cdot L^{-1}$ Na_2HPO_4, 2.452 $g \cdot L^{-1}$ $NaH_2PO_4 \cdot H_2O$, 0.31 $g \cdot L^{-1}$ NH_4Cl, 0.13 $g \cdot L^{-1}$ KCl), 5 mL vitamin solution, 12.5 mL mineral solution, and 1 g glucose (Tables 8, 9, and 10). A 500 mL volume of 50 mM potassium ferricyanide buffer was added into the cathode chamber. The two chambers were separated by a proton exchange membrane, and a 1000 ω resistance was connected externally to the chamber. The startup procedure was necessary to develop a working biofilm community on the anode for effective operation. The MFC startup was considered successful when the cell voltage reached a continuous output > 50 mV for two and a half successive cycles (each cycle = 200–300 h). After startup, the anode chamber substrate was replaced with fresh sediment for subsequent experimental measurements of electrical generation and methane emission. The anode chamber received 500 mL of sediment slurry (~ 172 g dry weight equivalent) and was allowed to settle naturally for 24 h. The cathode chamber contained 500 mL of either $K_3[Fe(CN)_6]$ or NaCl at concentrations ranging from 0 to 200 mM. All experimental treatments were performed in triplicate.

Electrical generation performance analysis

SMFCs were maintained at room temperature (~ 24 °C) with the output voltage recorded every 180 s by a data acquisition system (Model 2700, Keithley Inc., Solon, OH, USA). Polarization curves for the MFC were measured using the stable discharge method (Hong et al. 2009). Firstly, the external resistance was switched off so that an open circuit was formed; the open-circuit voltage was measured at this time. Then, the resistance was connected and voltages measured across decreasing resistance values from 90,000 to 100 Ω to calculate the homologous electric current density. Finally, polarization curves were developed from the data to estimate the internal cell resistance (Aelterman et al. 2006; Menicucci et al. 2006; Zhu et al. 2011). The power density of the MFC was calculated as:

$$P_{An} = U^2/(R_{ex} \bullet S_{An})$$

where P_{An} is the power density ($mW \cdot m^{-2}$); U is the output voltage (V); R_{ex} is the external resistance (Ω); and S_{An} is the shadow area of anode (m^2).

Quantification of methane and carbon dioxide emissions

During electrical production by the SMFCs, gases produced in the anode chamber were collected using an evacuated gas recovery bag (Zhang et al. 2016). The sealed anode chamber contained a glass orifice connected to the gas recovery bag with a latex tube. For each operational cycle, gas recovery bags collected the gases produced in the anode chamber. After each operational cycle was completed, we collected a 0.3 mL sample with a gas-tight syringe from the septum in the gas recovery bag for methane and CO_2 quantification. Their concentrations were measured by gas chromatography equipped with a flame ionization detector (HP 5890 Series II, Agilent Technologies, Santa Clara, USA). Total gas volume was determined by syringe evacuation/measurement of the gas recovery bag. The CO_2 emission fluxes (F) was calculated in the same manner as described for the methane emission fluxes (F). The methane emission fluxes (F) in the anode chamber were calculated as (Zhang et al. 2016):

$$F = (M \bullet P \bullet T_0 \bullet C \bullet V_1)/(V_0 \bullet P_0 \bullet T \bullet V_2 \bullet t)$$

where M is the molar mass of methane ($g \cdot mol^{-1}$); P is the atmospheric pressure (Pa); T is the temperature (K); V_0 is the molar volume of CH_4 at standard state ($mL \cdot mol^{-1}$); P_0 is the atmospheric pressure at standard state (Pa); T_0 is the absolute temperature at standard state (K); C is the gas concentration per volume (ppm_V); V_1 is the gas output in operational cycle (mL) = gas volume in recovery bag was measured by syringe evacuation; V_2 is the sediment slurry volume in the anode chamber (mL); and t is the duration of operational cycle (h).

Statistical analyses

We used Microsoft Office Excel 2007 to store and analyze the original data. Statistical differences among treatments were assessed using the nonparametric multiple paired rank sum test with mean separation by the Wilcoxon signed-rank test (two-tailed asymmetrical sign test). All statistical analyses were evaluated at a $p \leq 0.05$ level of significance using SPSS (V. 19.0) (IBM Inc., Foster City, CA, USA). Origin 8.5 (OriginLab, Northampton, MA, USA) was used to prepare graphics.

Results and discussion

Effect of cathode chamber electrolyte composition on MFC electrical generation

Effects of potassium ferricyanide concentration on MFC performance

The electron accepting capacity of the cathode is an important factor regulating the electrical generation performance of MFC systems (Rismani-Yazdi et al. 2008). As such, one would expect that the electrolyte composition would affect

overall MFC performance. Over the entire 600-h trial, mean power generation showed a general increase with increasing $K_3[Fe(CN)_6]$ concentrations from 0 to 150 mM, followed by a large decrease at 200 mM (Table 2), the latter drop off possibly due to enhanced consumption of ferricyanide in the cathode and nutrients in the anode medium. Another possibility was that the extrusion of potassium ferricyanide through PEM to anode chamber, osmotic pressure inhibited the movement of protons to the cathode chamber, decreasing the biodegradation of glucose (Wei et al. 2012). Differences in MFC voltage were most evident in the first ~ 300 h, whereafter the differences converged in the 300–600-h time period as the voltages of all MFCs dropped toward zero (Fig. 2). Initially (< 150 h), the voltage of the 0 mM $K_3[Fe(CN)_6]$ treatment lagged those treatments receiving $K_3[Fe(CN)_6]$. This was followed by a crossover point at ~ 150 h where the 0 mM $K_3[Fe(CN)_6]$ concentration had among the highest voltage outputs up to ~ 300 h, at which point the voltages of all treatments converged. Notable differences among the differing electrolyte concentrations included wide diel variability in the first 150 h for the 50 mM treatment and a distinctly elevated voltage for the 150 mM $K_3[Fe(CN)_6]$ treatment in the 100–300-h time period. Several treatments displayed a distinct diel pattern that we attribute to diurnal temperature variations associated with laboratory temperature fluctuations. Overall, even though the voltages displayed high variability within and among MFC treatments, the addition of $K_3[Fe(CN)_6]$ to a maximum concentration of 150 mM led to a faster voltage increase and somewhat more stable electrical output over the 600 h of investigation.

Polarization curves for the MFCs were obtained from data collected after the system reached stable operating conditions. Polarization curves showed systematic changes with increasing $K_3[Fe(CN)_6]$ concentrations in the cathode chamber (Fig. 3). As the $K_3[Fe(CN)_6]$ concentration was raised from 0 to 50–200 mM, the internal resistance of the MFCs showed a small reduction (1340 to 1303–1318 Ω), whereas maximum power densities showed a progressive increase from 4.50 to 6.45 $mW \cdot m^{-2}$ (Table 3). Wu et al. (2013) also found that the power density increased from 0.0276 to 2.1 mWm^{-2} as the concentration of potassium ferricyanide in the cathode chamber was increased from 0 to 200 mM (Wu et al. 2013). As with the temporal voltage

Table 2 SMFC voltage as a function of $K_3[Fe(CN)_6]$ concentration. Values with same letter are not significantly different at $p \leq 0.05$ as determined by Wilcoxon signed-rank test

$K_3[Fe(CN)_6]$ (mM)	Mean voltage (V)
0	0.462b
50	0.477c
100	0.471c
150	0.561d
200	0.436a

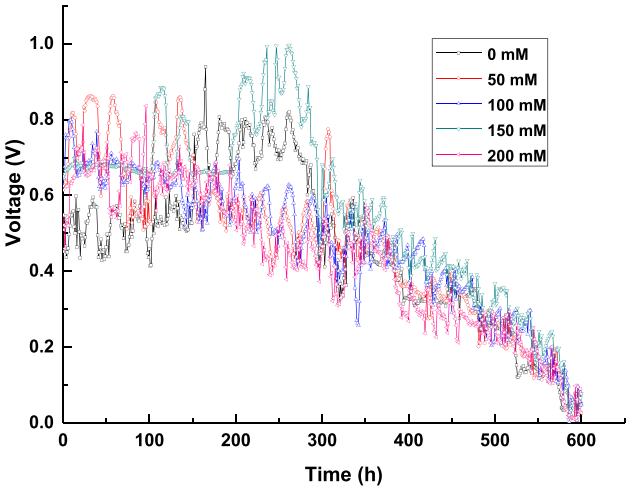

Fig. 2 Power generation of MFCs with different $K_3[Fe(CN)_6]$ concentrations in cathode chamber

outputs, the internal resistance showed a trend reversal as $K_3[Fe(CN)_6]$ concentration increased from 150 to 200 mM. These results demonstrate that the addition of $K_3[Fe(CN)_6]$ to the cathode chamber, which serves as an electrolyte and oxidizing agent, improves the electrical performance of the MFC system.

Under ambient conditions, dissolved oxygen (DO) serves as the electron acceptor in the cathode chamber and the DO concentration is regulated by exchange with the atmosphere. When $K_3[Fe(CN)_6]$ (not ferrocyanide, the reduced form) was added to the cathode chamber, both $K_3[Fe(CN)_6]$ and DO act as electron acceptors in the cathode region increasing reaction rates so that the output voltage reaches higher values more rapidly. In the cathode chamber, the ferricyanide ($Fe(CN)_6^{3-}$) was reduced to ferrocyanide ($Fe(CN)_6^{4-}$). The ferrocyanide is then oxidized in the cathode by oxygen to

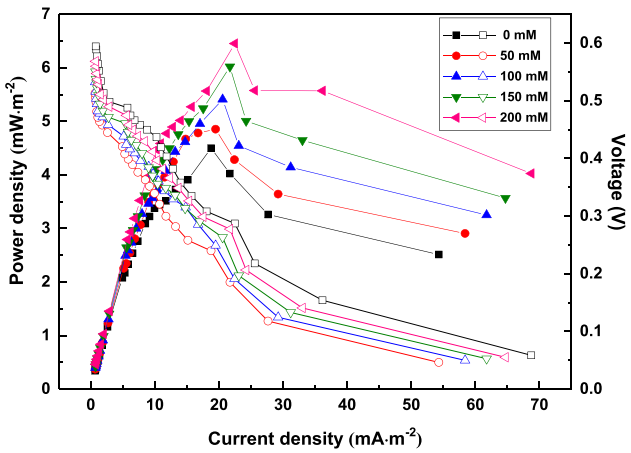

Fig. 3 Polarization curves (open symbols) and power density (solid symbols) of MFCs with different $K_3[Fe(CN)_6]$ concentrations

Table 3 Internal resistance and maximum power density of MFCs at different $K_3[Fe(CN)_6]$ concentrations

$K_3[Fe(CN)_6]$ concentration (mM)	0	50	100	150	200
Cell internal resistance (Ω)	1339.5	1318.0	1303.8	1303.1	1313.3
Maximum power density ($mW \cdot m^{-2}$)	4.50	4.85	5.41	6.02	6.45

form ferricyanide, which facilitates the reversibility of this reaction allowing easier cathodic reduction of the ferricyanide (as compared to oxygen reduction) (Penteado et al. 2017), thereby increasing the overall rate of electron transfer, such as:

$$O_2 + 4_H{}^+ + 4e^- \rightarrow 2H_2O$$
$$Fe(CN)_6{}^{3-} + e^- \rightarrow Fe(CN)_6{}^{4-}$$
$$O_2 + 4Fe(CN)_6{}^{4-} + 4H^+ \rightarrow 4Fe(CN)_6{}^{3-} + 2H_2O$$

Thus, when $K_3[Fe(CN)_6]$ is used as an electron acceptor in the cathode chamber, reaction rates with electrons are enhanced. Initially, the electron accepting rate is very high as an abundance of $Fe(CN)_6{}^{3-}$ is reduced to $Fe(CN)_6{}^{4-}$. However, the $Fe(CN)_6{}^{3-} \rightarrow Fe(CN)_6{}^{4-}$ reaction rate was not the main factor regulating the output current at the onset of the experimental trials (< 24 h), but rather the electron generation associated with the electrode biofilm. Following a transient adjustment period, the electrode biofilms begin to perform a more efficient series of reactions leading to electrical generation. As organic matter oxidation and electron generation progressed, $Fe(CN)_6{}^{3-}$ was progressively consumed and the electron accepting capacity of the cathode chamber decreased after ~ 300 h. Additionally, the supply of microbially labile organic substrates is depleted with increasing reaction times slowing microbial activity and electron/proton generation. As a result, the output voltage of the MFC demonstrated a decreasing trend over extended time periods.

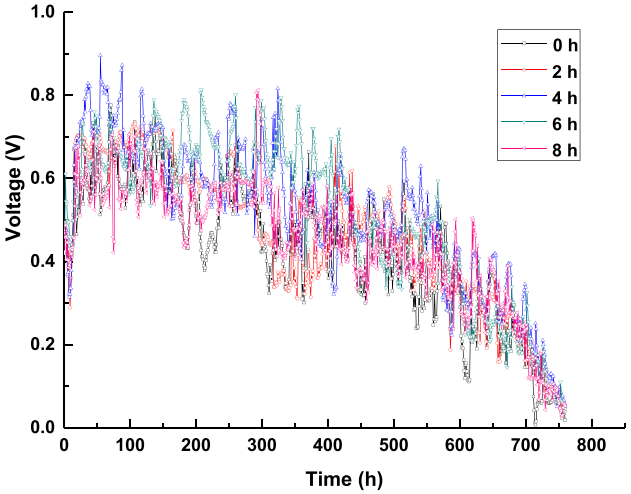

Fig. 4 Voltage profiles of MFCs as a function of daily aeration time

Table 4 MFC voltage as a function of cathode aeration time. Values with same letter are not significantly different at $p \leq 0.05$ as determined by Wilcoxon signed-rank test

Aeration time (h)	Mean voltage (V)
0 h	0.428a
2 h	0.463c
4 h	0.515e
6 h	0.508d
8 h	0.448b

Effects of aeration on MFC performance

Oxidizing agents in the cathode chamber act as electron acceptors in MFCs, reacting with electrons produced in the anode chamber to generate electrical production. Dissolved oxygen (DO) was the most common electron acceptor in the cathode chamber and it was a critical factor influencing microbial fuel cells (MFC) performance at cathodic interface (Rago et al. 2017). Therefore, we tested whether the efficiency of electrical production was improved by artificially aerating the cathode chamber to increase DO concentrations. Using 50 mM $K_3[Fe(CN)_6]$ as the cathode electrolyte and an internal resistance of 1000 Ω, the influence of cathode chamber aeration time (0 → 8 h/day) on electrical generation was assessed over a 760-h period (Fig. 4). After a ~ 24 h stabilization period, MFC voltages sharply increased and maintained a high voltage for ~ 400 h before trending downward to values of < 0.05 V at the termination of the trials. When assessing the entire 760-h period, aeration time significantly increased the SMFC voltage to a maximum value at 4 h (Table 4), after which time the voltage progressively tailed off as aeration increased to 6 and 8 h/day (Fig. 4).

Polarization curves and power densities were determined for MFCs receiving various aeration regimes once stable operating conditions were achieved (Fig. 5). Values for these parameters were very similar at current densities < 10 mA m^{-2}, but diverged at higher current densities. While there was no obvious trend for aeration effects on MFC internal resistances, the maximum power densities displayed a generally increasing trend with increasing aeration times (Table 5). Among the aeration treatments, the 6 h per day treatment demonstrated the largest increase relative to the reference cell receiving no artificial aeration, which reached 6.00 $mW \cdot m^{-2}$, but was lower than systems using $K_3[Fe(CN)_6]$ catholytes (6.45 $mW \cdot m^{-2}$). A possible reason for decreased performance at longer aeration times

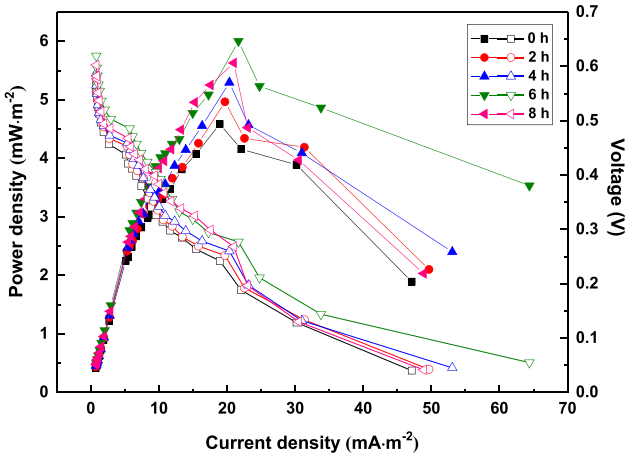

Fig. 5 Polarization curves (open symbols) and power densities (solid symbols) of MFCs as a function of daily aeration time

was oxygen intrusion into the anode chamber and impeded the anaerobic conditions necessary for microbial electron/proton generation (Lawson et al. 2020), which also explained that the maximum power density of 8-h aeration treatment being less than 6-h. These results demonstrate that DO augmentation to the cathode chamber has only a small relative effect on electrical production by MFCs. Electricity generation of the MFCs appears to be more strongly affected by the generation and transfer of electrons and protons from the oxidation of organic matter in the anode chamber (Oh &Logan 2006).

Effects of NaCl concentration on MFC performance

Sodium chloride was a common electrolyte used in the cathode chamber of MFCs to increase the electric conductivity of the anolyte and catholyte, thereby enhancing ionic strength and power output (Liu et al. 2005, Ramya &Senthil Kumar 2022). Thus, the salinity of the electrolyte must be as high as possible to decrease the ohmic drop, but it also must not exceed the level that microorganisms can tolerate (Rousseau et al. 2013). Sodium chloride concentration in the cathode chamber was increased from 0 → 200 mM and the voltage monitored over 640 h of operation. A maximum mean voltage was achieved at 100 mM NaCl and then diminished at higher concentrations (Table 6). Most treatments showed an initial increase in voltage to a maximum value within 100–200 h (Fig. 6). Maximum voltages approaching 1 V were quickly achieved for the 100 and 150 mM treatments, but the 150 mM treatment experienced a rapid decrease in voltage at ~ 100 h, whereas the higher

Table 6 MFC voltage as a function of cathode NaCl concentration. Values with same letter are not significantly different at $p \leq 0.05$ as determined by Wilcoxon signed-rank test

NaCl (mM)	Mean voltage (V)
0	0.481b
50	0.475b
100	0.717c
150	0.471b
200	0.377a

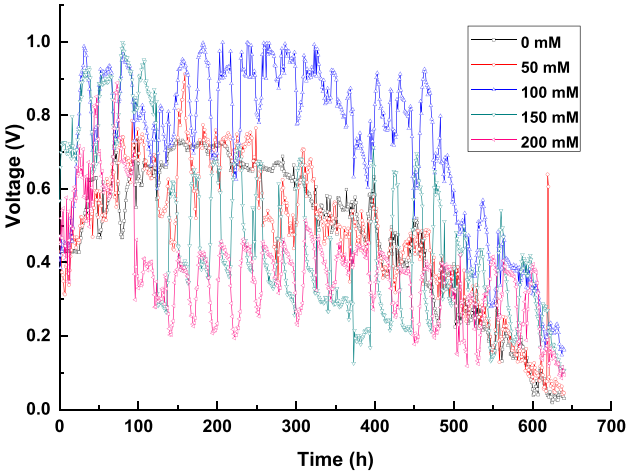

Fig. 6 Power generation of MFCs with different NaCl concentration in cathode chamber

voltages were maintained for ~ 450 h in the 100 mM treatment. These experimental trials demonstrate that the addition of NaCl to the cathode chamber at an optimal concentration can substantially improve MFC electricity production efficiency and maximal voltage levels. For our experimental system, the 100 mM NaCl concentration produced the best cathode electrolyte for electrical generation, whereas the lower and higher NaCl concentrations resulted in lower electrical generation.

Polarization curves and power densities were measured for MFC at various NaCl concentrations once the systems reached stable operating conditions. Values for these parameters were very similar at current densities < 10 mA m^{-2}, but became progressively differentiated as current densities increased (Fig. 7). The internal resistance of the MFCs showed a progressive decrease while the maximum power density increased as NaCl concentrations increased from 0 to 200 mM (Table 7). These changes occurred because the conductivity of the cathode

Table 5 MFC resistances and maximum power densities as a function of daily aeration time

Aeration time (h)	0	2	4	6	8
Cell internal resistance (Ω)	1330.1	1340.1	1290.4	1303.6	1316.3
Maximum power density (mW·m^{-2})	4.59	4.96	5.30	6.00	5.63

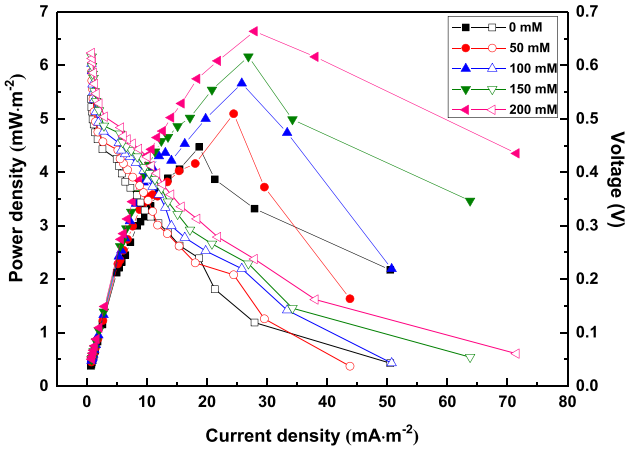

Fig. 7 Polarization curve (open symbols) and power densities (solid symbols) with different NaCl concentration in cathode chamber

chamber increased, thereby reducing the internal resistance, which in turn increased electron and proton transfer.

When comparing $K_3[Fe(CN)_6]$ vs NaCl at the same concentrations, we found that NaCl had a greater effect in decreasing the internal resistance of the system. In contrast, $K_3[Fe(CN)_6]$ did not decrease the internal cell resistance, but did increase the power generation capacity though its dual roles as an electrolyte and electron acceptor. Power density is a function of the combination of cell voltage and resistance (i.e., $P_{An} = U^2/(R_{ex} \cdot S_{An})$). Thus, the higher U (output voltage) resulting from using $K_3[Fe(CN)_6]$ in the cathode was more critical to power generation than the slightly higher internal resistance (Lawson et al. 2020). Furthermore, Wei and coworkers found some leakage of ferricyanide through the PEM to the anode chamber that resulted in osmotic pressure inhibition. This osmotic pressure inhibition impeded the movement of protons to the cathode chamber, thereby decreasing the biodegradation of organic matter (Wei et al. 2012).

Effects of cathode chamber composition on total gas and CH_4 production

Effects of potassium ferricyanide concentration on total gas and CH_4 production

The release of electrons from organic matter degradation in the anode chamber results in the production of several gaseous products, most notably CO_2 and CH_4, but also trace levels of N_2O, NO, N_2, H_2S, and H_2 (Pitombo et al. 2018). Total gas production and methane emission fluxes from the anode chamber showed a distinct increase compared to the reference condition (RC) having no electrical generation (no cathode/anode connection) (Fig. 9). With increasing $K_3[Fe(CN)_6]$ concentrations (0 → 200 mM) in the cathode chamber, total gas production displayed a slightly increasing trend, whereas CH_4 emission showed a pronounced decreasing trend ($181.6 \pm 10.9 \rightarrow 75.5 \pm 9.7$ mg/m^3·h). The CO_2:CH_4molar ratio of gas emissions showed an increase from 19.3 to 51.8 at 0 and 200 mM $K_3[Fe(CN)_6]$, respectively, as compared to 74.1 for the reference condition (Table S4). Addition of $K_3[Fe(CN)_6]$, an electron acceptor, to the cathode chamber promoted electron transfer from the anode to cathode chamber. As a result, organic matter degradation in the anode chamber was enhanced resulting in greater gas production via anaerobic metabolic processing. However, the more efficient transport of electrons from the anode decreased the availability of electrons to participate in methane production. As a result, the yield of CO_2 concentrations increased at the expense of decreasing CH_4 concentrations (Table S4). Notably, both total gas production and methane emission were greatly suppressed under reference conditions (RC) having no electrical generation.

Effects of aeration on total gas and CH4 production

Aeration of the cathode chamber had little effect on total gas volume or methane emission fluxes in the anode chamber (Fig. 10). However, both total gas volumes and methane emissions where appreciably higher in the non-aerated treatment with electrical production (0 h treatment) than in the reference condition (RC) having no electrical generation. This indicates that electrical generation associated with biofilms on the anode accelerates organic matter transformation processes and methane emission. Among aeration treatments, CH_4 emission from the 6-h treatment was significantly ($p \leq 0.05$) less than that of non-aerated treatment (0 h). Notably, the 6-h aeration treatment had the highest power density among aeration treatments (Fig. 5 and Table 5). This suggests an inverse relationship between methane emission flux and power density owing to the more efficient transport of electrons from the anode to cathode at higher power densities. When comparing the effects of aeration (DO) versus $K_3[Fe(CN)_6]$ concentrations in the cathode (both electron acceptors), we infer that $K_3[Fe(CN)_6]$ concentration is a more important factor than

Table 7 Cell internal resistance and power density with different NaCl concentration in cathode chamber

NaCl concentration (mM)	0	50	100	150	200
Cell internal resistance (Ω)	1321.6	1279.7	1247.5	1186.8	1140.4
Maximum power density (mW·m^{-2})	4.47	5.09	5.67	6.16	6.64

aeration in promoting electron transfer from the anode to cathode (Raghavulu et al. 2009).

Effects of NaCl on total gas and CH4 production

Increasing NaCl concentrations in the cathode chamber resulted in increasing total gas volumes and a decrease in methane generation (Fig. 11). The higher power densities found at higher NaCl concentrations (Table 6) indicate that higher electrolyte concentrations enhance microbial degradation of organic matter (i.e., greater gas production) and decrease methane generation by facilitating electron transfer from the anode to cathode chambers. At similar electrolyte concentrations, total gas generation was similar between NaCl and $K_3[Fe(CN)_6]$ treatments (~ 70–80 mL); however, methane production was about twice as high for NaCl (~ 150–400 mg/m^3·h) compared to $K_3[Fe(CN)_6]$ (~ 75–175 mg/m^3·h) (Figs. 9 and 11). We attribute the decreased CH_4 generation in the $K_3[Fe(CN)_6]$ versus NaCl systems to greater electron transfer efficiency as $K_3[Fe(CN)_6]$ acts an electron acceptor.

Relationship between electrical generation and methane production in MFC

Under anaerobic conditions, methane production in the anode chamber of MFCs results from decomposition of organic matter by methanogenic bacteria in the sediments through a series of redox processes. The activity of biofilm communities determines the amount of gas and types of gaseous products generated (Vu &Min 2019). Power density is a critical term that characterizes the activity of electricigens (i.e., microorganisms that oxidize organic compounds and transfer electrons to the anode). Microbial communities generating higher power densities have a higher capacity for degradation/transformation of organic compounds. Thus, a higher biofilm activity promotes organic matter degradation and increases the volume of gases produced (Yang et al. 2015). Application of MFC systems in organic-rich sediment could provide environmental benefits such as decreasing organic matter (including organic pollutants and sediment oxygen demand) and attenuating methane emission in conjunction with electricity production via anaerobic degradation processes (Hong et al. 2009).

Under different chemical environments in the cathode chamber, gas volumes produced in the anode chamber of the MFC tended to increase as power densities increased. In all cases, the process of electrical generation clearly increased total gas volumes compared to the reference condition (RC) having no cathode/anode electrode connection. The diversity of bacterial and archaea communities was analyzed in SMFC using the same sediments in our previous study (Zhu et al. 2016). We have found that the predominant bacterium at the phylum level was *Proteobacteria*, which was known to be dominant in MFCs due to their ability to donate electrons (Almatouq et al. 2020; Kabutey et al. 2019a, b; Xie et al. 2017). At the genus level, *Geobacter* was predominant, which can via outer membrane cytochrome (OMCs) to accomplish direct electron transfer (DET) that contributed to higher current densities in MFCs (Aiyer 2020). The electrode participation increased the abundance of electricigen bacteria (e.g., *Geobacter*, *Pseudomonas*, and *shewanella*) in the biofilm community (Wu et al. 2019, Yang &Chen 2021), which increases electrical generation by enhancing organic matter transformations in the sediment substrate with correspondingly higher gas generation. Yu et al. (2018) demonstrated that higher densities of *Geobacter* on the anode resulted in enhanced electrogenic performance (Yu et al. 2018). Notably, methane generation was significantly higher for electrical-generating treatments than for the reference condition (RC) having no electrical generation. This becomes an important concern as the global warming potential of CH_4 is ~ 28 times higher than CO_2 over a 100 year period (Myhre et al. 2013).

Suppression of methane production is a major challenge for achieving the practical application of several types of bioelectrochemical systems. Methane formation occurs under specific biogeochemical conditions, such as redox potential (Eh), pH, and ammonia concentration (Arends et al. 2014). Hence, it is warranted to assess mitigation strategies to attenuate CH_4 generation during MFC operation (Chae et al. 2010). In an MFC cathode, the oxygen concentration and reduction capacity are the main limiting factors on electricity generation performance of MFCs, so it is necessary to increase the electron-accepting/transfer capacity of the cathode. For example, *Chlorella vulgaris* was added to the cathode chamber to produce oxygen as an electron acceptor (Song et al. 2020). Alternatively, HF gas transfer membranes were used to transfer pure oxygen to the cathode chamber to provide enhanced cathode ventilation to increase electron accepting capacity (Taşkan 2020). In this study, electron-accepting/transfer capacity was increased by adding sodium chloride and potassium ferricyanide to the cathode or by aeration. An assessment of our treatment groups ($K_3[Fe(CN)_6]$, NaCl, and aeration) showed a strong inverse relationship between power densities and CH_4 emission flux (Fig. 8). Thus, optimizing cathode chemical composition to enhance electron-accepting/transfer capacity demonstrates potential for increasing electrical generation while simultaneously reducing CH_4 emission from MFCs.

Methane generation from sediments in the anode is primarily influenced by the activity of methanogenic bacteria, labile organic substrates in the sediment, and proton/electron transfer capacity of the system. Methane is produced mainly through methanogenesis reactions: (1) $\text{acetate}^- + H^+ \rightarrow CH_4 + CO_2$ (acetoclastic), and (2)

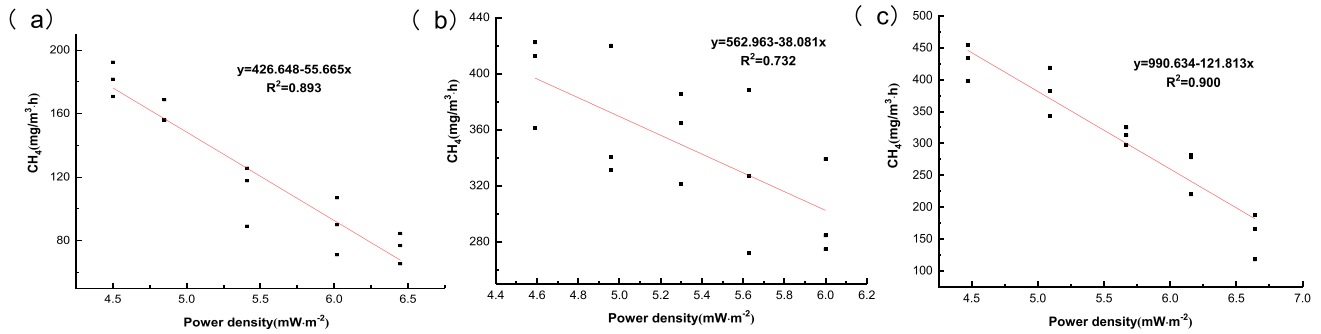

Fig. 8 Relationship between power density and methane emission fluxes for $K_3[Fe(CN)_6]$ (left panel), aeration (middle panel), and NaCl (right panel) treatments within the cathode chamber

$4H_2 + CO_2 \rightarrow CH_4 + 2H_2O$ (hydrogenotrophic). Therefore, the products of anodic organic degradation (H_2 and/or acetate) are necessary substrates for methanogens. Similarly, electrical generation is carried out primarily via the hydrogen and acetate substrates produced by fermentative organisms (Freguia et al. 2008). We have found that the archaeal community showed a higher presence of *Euryarchaeota* at the phylum level, and at the genus level, *Methanosaeta* and *Candidatus Methanoregula* were abundant, followed by *Methanobacterium* (Zhu et al. 2016). Hence, within MFCs, electricigens and methanogenic bacteria compete with each other for labile organic substrates, as well as proton transfer (Chung et al. 2019; Xu et al. 2021a, b). Higher power densities in each treatment group represent a higher activity of electricigens, more degradation of organic substrates and more efficient transfer of protons. Higher electricigen activities have a suppressive effect by competing with methanogenic bacteria for protons and primary/intermediate organic substrates. Hence, the higher electricigen activities lead to higher power densities, while also leading to lower methane emission. This suppressive phenomenon (competition) between electricigen and methanogenic bacteria may also have a negative impact on the efficiency of electrical generation by MFC systems (Rozendal et al. 2008). Electricigen bacteria outcompete methanogenic bacteria at low organic carbon concentrations (electron donor) and high electron acceptor concentrations (anode in closed circuit) (Arends et al. 2014). Therefore, in our experimental trials, as the concentration of electron acceptors increased in the cathode, methane generation was suppress and power generation efficiency increased.

We further examined the relationship CO_2:CH_4 molar ratio of gas emissions as a function of $K_3[Fe(CN)_6]$ concentrations in the cathode chamber (Table S4). The CO_2:CH_4 ratio of the $K_3[Fe(CN)_6]$ treatment groups was higher than that of the reference condition. As biochemical reactions and electron production are much slower under the reference condition with no electrode connection (i.e., lower overall gas production), it is likely that intermediate substrate formation (e.g., H_2 and CH_3COOH) is hindered, as well as carbon dioxide reduction to methane, thereby leading to a higher CO_2:CH_4 ratio under the reference condition. As the concentration of $K_3[Fe(CN)_6]$ increased in the operational MFCs, CO_2 generation showed a slightly increasing trend while CH_4 production dropped by greater than twofold. We attribute this pattern of decreasing CH_4 production to competition for electrons and substrates (e.g., H_2 and CH_3COOH) between methanogens and electricigens, in which electricigens have a competitive advantage as electrons are shuttled to the cathode through the electrical circuit. Furthermore, *Methanobacterium* may reverse the electromethanogenesis process and donated electrons to the anode resulting in methane consumption (McAnulty et al. 2017). When assessing our cathode chamber treatment groups ($K_3[Fe(CN)_6]$, NaCl, and aeration), the higher power densities ascribed to higher electrogenesis lead to greater suppression/competition with methanogens resulting in a decreased methane emission flux. Thus, optimizing conditions to achieve higher power densities through cathode (increasing electron accepting and conductivity parameters) and anode (altering organic substrates) amendments has the potential to enhance electrical generation while suppressing CH_4 production.

Conclusion

This study assessed alteration of cathode chamber chemistry in a two-compartment SMFC to optimize power generation and minimize methane production. The efficiency of the SMFCs was mainly determined by the chemical environment of the cathode chamber and substrate composition of the anode chamber. In the operation cycles employing aeration and $K_3[Fe(CN)_6]$ addition to the cathode chamber, internal resistances were similar with values of ~ 1300 Ω. Power densities of SMFCs reached maximum

values at 150 mM $K_3[Fe(CN)_6]$ and 6 h/day aeration time in the cathode chamber, with corresponding maximum power densities of 6.45 and 6.00 $mW \cdot m^{-2}$, respectively. The addition of an electron acceptor ($K_3[Fe(CN)_6]$) in the cathode chamber improved the electricity generation efficiency of the SMFC, but did not change the internal resistance of the SMFC. Increasing NaCl concentrations in cathode chamber decreased the internal cell resistance and increased the efficiency of electricity generation. Maximum power density (6.64 $mW \cdot m^{-2}$) occurred at a NaCl concentration of 200 mM with a corresponding internal resistance of 1140.4 Ω. Increasing the concentration of $K_3[Fe(CN)_6]$ or NaCl, or extending the aeration time in cathode chamber, resulted in increased gas production (reflecting higher microbial activity) in the anode chamber. The gas volume and methane emission in the treatment groups were significantly higher than that in the reference control indicating the role of the electrodes (specifically the electrode biofilm communities) in enhancing microbial activity and gas production rates in the anode sediment. Methane emission showed a distinct decrease as the efficiency of electrical generation increased, displaying a strong negative correlation between power densities and methane emission flux. Thus, optimizing cathode chemical conditions can simultaneously increase electrical production efficiency and pollutant degradation while decreasing methane emission during SMFC treatment of anaerobic sediments.

Supplementary Information The online version contains supplementary material available at https://doi.org/10.1007/s11356-022-19292-x.

Acknowledgements The authors would like to acknowledge financial support for this work provided by the Ministry of Science and Technology of China for State Key Research and Development Project (2016YFC0400702), and the Science and Technology Planning Project of Shaoguang City, Guangdong Province, China (2019CS05307).

Author contribution Methodology, conceptualization, and investigation were performed by YY and TPZ. JHX was in charge of writing-original draft and writing-review and editing. FJH was mainly responsible for resources for this article. Supervision was performed by RAD and TPZ. All authors commented on previous versions of the manuscript. All authors read and approved the final manuscript.

Funding Partial financial support was received from the Ministry of Science and Technology of China for State Key Research and Development Project (2016YFC0400702), and the Science and Technology Planning Project of Shaoguang City, Guangdong Province, China (2019CS05307).

Data Availability Not applicable.

Declarations

Ethics approval and consent to participate Not applicable.

Consent for publication Not applicable.

Competing interests The authors declare no competing interests.

References

Abbas SZ, Rafatullah M, Ismail N, Syakir MI (2017) A review on sediment microbial fuel cells as a new source of sustainable energy and heavy metal remediation; mechanisms and future prospective. INT J ENERG RES 41:1242–1264

Aelterman P, Rabaey K, Pham HT, Boon N, Verstraete W (2006) Continuous electricity generation at high voltages and currents using stacked microbial fuel cells. ENVIRON SCI TECHNOL 40:3388–3394

Ahn Y, Hatzell MC, Zhang F, Logan BE (2014) Different electrode configurations to optimize performance of multi-electrode microbial fuel cells for generating power or treating domestic wastewater. J POWER SOURCES 249:440–445

Aiyer KS (2020) How does electron transfer occur in microbial fuel cells? WORLD J MICROB BIOT 36:19–19

Almatouq A, Babatunde AO, Khajah M, Webster G, Alfodari M (2020) Microbial community structure of anode electrodes in microbial fuel cells and microbial electrolysis cells. Journal of Water Process Engineering 34:101140

Arends JBA, Speeckaert J, Blondeel E, De Vrieze J, Boeckx P, Verstraete W, Rabaey K, Boon N (2014) Greenhouse gas emissions from rice microcosms amended with a plant microbial fuel cell. APPL MICROBIOL BIOT 98:3205–3217

Bond DR (2002) Electrode-reducing microorganisms that harvest energy from marine sediments. Science 295:483–485

Cai J, Zheng P, Mahmood Q (2016) Effect of cathode electron acceptors on simultaneous anaerobic sulfide and nitrate removal in microbial fuel cell. WATER SCI TECHNOL 73:947–954

Catal T, Li K, Bermek H, Liu H (2008) Electricity production from twelve monosaccharides using microbial fuel cells. J POWER SOURCES 175:196–200

Chae K, Choi M, Kim K, Ajayi FF, Park W, Kim C, Kim IS (2010) Methanogenesis control by employing various environmental stress conditions in two-chambered microbial fuel cells. BIORESOURCE TECHNOL 101:5350–5357

Chakraborty I, Bhowmick GD, Ghosh D, Dubey BK, Pradhan D, Ghangrekar MM (2020) Novel low-cost activated algal biochar as a cathode catalyst for improving performance of microbial fuel cell. Sustainable Energy Technologies and Assessments 42:100808

Chung R, Kang EY, Shin YJ, Park JJ, Park PS, Han CH, Kim B, Moon SI, Park J, Chung PS (2019) Development of a consolidated anaerobic digester and microbial fuel cell to produce biomethane and electricity from cellulosic biomass using bovine rumen microorganisms. Journal of Sustainable Bioenergy Systems 09:17–28

Dai HY, Yang HM, Liu X, Zhao Y, Liang ZH (2016) Performance of sodium bromate as cathodic electron acceptor in microbial fuel cell. BIORESOURCE TECHNOL 202:220–225

Elshobary ME, Zabed HM, Yun J, Zhang G, Qi X (2021) Recent insights into microalgae-assisted microbial fuel cells for generating sustainable bioelectricity. INT J HYDROGEN ENERG 46:3135–3159

Erbay C, Yang G, de Figueiredo P, Sadr R, Yu C, Han A (2015) Three-dimensional porous carbon nanotube sponges for high-performance anodes of microbial fuel cells. J POWER SOURCES 298:177–183

Ewing T, Ha PT, Babauta JT, Tang NT, Heo D, Beyenal H (2014) Scale-up of sediment microbial fuel cells. J POWER SOURCES 272:311–319

Freguia S, Rabaey K, Yuan Z, Keller J (2008) Syntrophic processes drive the conversion of glucose in microbial fuel cell anodes. ENVIRON SCI TECHNOL 42:7937–7943

Greenman J, Gajda I, Ieropoulos I (2019) Microbial fuel cells (MFC) and microalgae; photo microbial fuel cell (PMFC) as complete recycling machines. SUSTAIN ENERG FUELS 3:2546–2560

Hong SW, Chang IS, Choi YS, Kim BH, Chung TH (2009) Responses from freshwater sediment during electricity generation using microbial fuel cells. BIOPROC BIOSYST ENG 32:389–395

Hong SW, Kim HS, Chung TH (2010) Alteration of sediment organic matter in sediment microbial fuel cells. ENVIRON POLLUT 158:185–191

Inoue K, Ito T, Kawano Y, Iguchi A, Miyahara M, Suzuki Y, Watanabe K (2013) Electricity generation from cattle manure slurry by cassette-electrode microbial fuel cells. J BIOSCI BIOENG 116:610–615

Kabutey FT, Zhao Q, Wei L, Ding J, Antwi P, Quashie FK, Wang W (2019a) An overview of plant microbial fuel cells (PMFCs): configurations and applications. Renew Sustain Energy Rev 110:402–414

Kabutey FT, Ding J, Zhao Q, Antwi P, Quashie FK, Tankapa V, Zhang W (2019b) Pollutant removal and bioelectricity generation from urban river sediment using a macrophyte cathode sediment microbial fuel cell (mSMFC). Bioelectrochemistry 128:241–251

Kodali M, Herrera S, Kabir S, Serov A, Santoro C, Ieropoulos I, Atanassov P (2018) Enhancement of microbial fuel cell performance by introducing a nano-composite cathode catalyst. ELECTROCHIM ACTA 265:56–64

Lawson K, Rossi R, Regan JM, Logan BE (2020) Impact of cathodic electron acceptor on microbial fuel cell internal resistance. BIORESOURCE TECHNOL 316:123919

Liang ZW, Siegert M, Fang WW, Sun Y, Jiang F, Lu H, Chen GH, Wang SQ (2017) Blackening and odorization of urban rivers: a bio-geochemical process. FEMS MICROBIOL ECOL 94:fix 180

Liu H, Cheng SA, Logan BE (2005) Power generation in fed-batch microbial fuel cells as a function of ionic strength, temperature, and reactor configuration. ENVIRON SCI TECHNOL 39:5488–5493

Logan B, Cheng SA, Watson V, Estadt G (2007) Graphite fiber brush anodes for increased power production in air-cathode microbial fuel cells. ENVIRON SCI TECHNOL 41:3341–3346

Logan BE, Rossi R, Ragab A, Saikaly PE (2019) Electroactive microorganisms in bioelectrochemical systems. Nat Rev Microbiol 17:307–319

Lovley DR (2006) Bug juice: harvesting electricity with microorganisms. NAT REV MICROBIOL 4:497–508

Lowy DA, Tender LM, Zeikus JG, Park DH, Lovley DR (2006) Harvesting energy from the marine sediment–water interface II. Biosens Bioelectron 21:2058–2063

McAnulty MJ, G. Poosarla V, Kim K, Jasso-Chávez R, Logan BE, Wood TK (2017) Electricity from methane by reversing methanogenesis. NAT COMMUN 8:15419

Menicucci J, Beyenal H, Marsili E, Veluchamy DG, Lewandowski Z (2006) Procedure for determining maximum sustainable power generated by microbial fuel cells. ENVIRON SCI TECHNOL 40:1062–1068

Miyahara M, Kouzuma A, Watanabe K (2015) Effects of NaCl concentration on anode microbes in microbial fuel cells. AMB Express 5:34

Myhre G, Shindell D, Bréon FM, Collins W, Fuglestvedt J, Huang J, Koch D, Lamarque JF, Lee D, Mendoza B, Nakajima T, Robock A, Stephens G, Takemura T, Zhang H (2013) Anthropogenic and natural radiative forcing. In: Stocker TF, Qin D, Plattner GK, Tignor M, Allen SK, Boschung J, Nauels A, Xia Y, Bex V, Midgley PM (eds) Climate change 2013: the physical science basis. Contribution of working group I to the fifth assessmentreport of the intergovernmental panel on climate change. Cambridge University Press, Cambridge, pp 659–740

Oh S, Logan BE (2006) Proton exchange membrane and electrode surface areas as factors that affect power generation in microbial fuel cells. APPL MICROBIOL BIOT 70:162–169

Penteado ED, Fernandez-Marchante CM, Zaiat M, Gonzalez ER, Rodrigo MA (2017) On the effects of ferricyanide as cathodic mediator on the performance of microbial fuel cells. ELECTROCATALYSIS-US 8:59–66

Pitombo LM, Ramos JC, Quevedo HD, Do Carmo KP, Paiva JMF, Pereira EA, Do Carmo JB (2018) Methodology for soil respirometric assays: step by step and guidelines to measure fluxes of trace gases using microcosms. MethodsX 5:656–668

Raghavulu SV, Mohan SV, Goud RK, Sarma PN (2009) Effect of anodic pH microenvironment on microbial fuel cell (MFC) performance in concurrence with aerated and ferricyanide catholytes. ELECTROCHEM COMMUN 11:371–375

Rago L, Cristiani P, Villa F, Zecchin S, Colombo A, Cavalca L, Schievano A (2017) Influences of dissolved oxygen concentration on biocathodic microbial communities in microbial fuel cells. Bioelectrochemistry 116:39–51

Ramya M, Senthil Kumar P (2022) A review on recent advancements in bioenergy production using microbial fuel cells. CHEMOSPHERE 288:132512

Rismani-Yazdi H, Carver SM, Christy AD, Tuovinen OH (2008) Cathodic limitations in microbial fuel cells: an overview. J POWER SOURCES 180:683–694

Rizzo A, Boano F, Revelli R, Ridolfi L (2013) Can microbial fuel cells be an effective mitigation strategy for methane emissions from paddy fields? ECOL ENG 60:167–171

Rosenbaum M, Zhao F, Schröder U, Scholz F (2006) Interfacing electrocatalysis and biocatalysis with tungsten carbide: a high-performance, noble-metal-free microbial fuel cell. Angew Chem Int Ed 45:6658–6661

Rosenbaum M, Zhao F, Quaas M, Wulff H, Schröder U, Scholz F (2007) Evaluation of catalytic properties of tungsten carbide for the anode of microbial fuel cells. Appl Catal B 74:261–269

Rousseau R, Dominguez-Benetton X, Délia M, Bergel A (2013) Microbial bioanodes with high salinity tolerance for microbial fuel cells and microbial electrolysis cells. ELECTROCHEM COMMUN 33:1–4

Rozendal RA, Hamelers HVM, Rabaey K, Keller J, Buisman CJN (2008) Towards practical implementation of bioelectrochemical wastewater treatment. TRENDS BIOTECHNOL 26:450–459

Shen J, Du ZP, Li JF, Cheng FQ (2020) Co-metabolism for enhanced phenol degradation and bioelectricity generation in microbial fuel cell. Bioelectrochemistry (Amsterdam, Netherlands) 134:107527

Sindhuja M, Harinipriya S, Bala AC, Ray AK (2018) Environmentally available biowastes as substrate in microbial fuel cell for efficient chromium reduction. J HAZARD MATER 355:197–205

Song XS, Wang WT, Cao X, Wang YH, Zou LX, Ge XY, Zhao YF, Si ZH, Wang YF (2020) Chlorella vulgaris on the cathode promoted the performance of sediment microbial fuel cells for electrogenesis and pollutant removal. SCI TOTAL ENVIRON 728:138011

Taşkan B (2020) Increased power generation from a new sandwich-type microbial fuel cell (ST-MFC) with a membrane-aerated cathode. Biomass and Bioenergy 142:105781

Tatinclaux M, Gregoire K, Leininger A, Biffinger JC, Tender L, Ramirez M, Torrents A, Kjellerup BV (2018) Electricity generation from wastewater using a floating air cathode microbial fuel cell. Water-Energy Nexus 1:97–103

Ucar D, Zhang Y, Angelidaki I (2017) An overview of electron acceptors in microbial fuel cells. FRONT MICROBIOL 8:643

Verma J, Kumar D, Singh N, Katti SS, Shah YT (2021) Electricigens and microbial fuel cells for bioremediation and bioenergy production: a review. ENVIRON CHEM LETT 19:2091–2126

Vu HT, Min B (2019) Integration of submersible microbial fuel cell in anaerobic digestion for enhanced production of methane and current at varying glucose levels. INT J HYDROGEN ENERG 44:7574–7582

Wang CT, Sangeetha T, Zhao F, Garg A, Chang CT, Wang CH (2018) Sludge selection on the performance of sediment microbial fuel cells. INT J ENERG RES 42:4250–4255

Wang HM, Ren ZJ (2014) Bioelectrochemical metal recovery from wastewater: a review. WATER RES 66:219–232

Wang SQ, Tian S, Zhang PY, Ye JP, Tao X, Li F, Zhou ZY, Nabi M (2019) Enhancement of biological oxygen demand detection with a microbial fuel cell using potassium permanganate as cathodic electron acceptor. J ENVIRON MANAGE 252:109682

Wei LL, Han HL, Shen JQ (2012) Effects of cathodic electron acceptors and potassium ferricyanide concentrations on the performance of microbial fuel cell. INT J HYDROGEN ENERG 37:12980–12986

Wu CH, Lai CY, Lin CW, Kao MH (2013) Generation of power by microbial fuel cell with ferricyanide in biodegradation of benzene. Clean: Soil, Air, Water 41:390–395

Wu MS, Xu X, Lu KX, Li XQ (2019) Effects of the presence of nanoscale zero-valent iron on the degradation of polychlorinated biphenyls and total organic carbon by sediment microbial fuel cell. SCI TOTAL ENVIRON 656:39–44

Xie BH, Gong WJ, Ding A, Yu HR, Qu FS, Tang XB, Yan ZS, Li GB, Liang H (2017) Microbial community composition and electricity generation in cattle manure slurry treatment using microbial fuel cells: effects of inoculum addition. ENVIRON SCI POLLUT R 24:23226–23235

Xu C, Poon K, Choi MMF, Wang RH (2015) Using live algae at the anode of a microbial fuel cell to generate electricity. ENVIRON SCI POLLUT R 22:15621–15635

Xu H, Song HL, Singh RP, Yang YL, Xu JY, Yang XL (2021) Simultaneous reduction of antibiotics leakage and methane emission from constructed wetland by integrating microbial fuel cell. BIORESOURCE TECHNOL 320:124285

Xu JY, Xu H, Yang XL, Rajendra PS, Li T, Wu Y, Song HL (2021b) Simultaneous bioelectricity generation and pollutants removal of sediment microbial fuel cell combined with submerged macrophyte. INT J HYDROGEN ENERG 46:11378–11388

Yang XN, Chen SS (2021) Microorganisms in sediment microbial fuel cells: Ecological niche, microbial response, and environmental function. SCI TOTAL ENVIRON 756:144145

Yang Y, Wang J, Zhu JP, Zhang TP (2015) Electricity generation by urban black smelly river sediment-MFC and the effect on sediment remediation. ECOL ENVIRON SCI 24:463–468

Yilmazel YD, Zhu X, Kim K, Holmes DE, Logan BE (2018) Electrical current generation in microbial electrolysis cells by hyperthermophilic archaea Ferroglobus placidus and Geoglobus ahangari. Bioelectrochemistry (amsterdam, Netherlands) 119:142–149

You SJ, Zhao QL, Zhang JN, Jiang JQ, Zhao SQ (2006) A microbial fuel cell using permanganate as the cathodic electron acceptor. J POWER SOURCES 162:1409–1415

Yu LP, Yang ZJ, He QX, Zeng RJ, Bai YN, Zhou SG (2018) Novel gas diffusion cloth bioanodes for high-performance methane-powered microbial fuel cells. ENVIRON SCI TECHNOL 53:530–538

Zhang TP, Huang XY, Yang Y, Li YL, Dahlgren RA (2016) Spatial and temporal variability in nitrous oxide and methane emissions in urban riparian zones of the Pearl River Delta. ENVIRON SCI POLLUT R 23:1552–1564

Zhong WH, Cai LC, Wei ZG, Xue HJ, Han C, Deng H (2017) The effects of closed circuit microbial fuel cells on methane emissions from paddy soil vary with straw amount. CATENA 154:33–39

Zhu JP, Wang J, Zhang TP, Zhu NW, Zou DH (2016) Phylogenetic diversity of bacterial and archaeal communities in anode biofilm of sediment microbial fuel cells. Acta Sci Circum 36:4017–4024

Zhu JP, Zhang TP, Zhu NW, Feng CH, Zhou SQ, Dahlgren RA (2019) Bioelectricity generation by wetland plant-sediment microbial fuel cells (P-SMFC) and effects on the transformation and mobility of arsenic and heavy metals in sediment. ENVIRON GEOCHEM HLTH 41:2157–2168

Zhu NW, Chen X, Zhang T, Wu PX, Li P, Wu JH (2011) Improved performance of membrane free single-chamber air-cathode microbial fuel cells with nitric acid and ethylenediamine surface modified activated carbon fiber felt anodes. BIORESOURCE TECHNOL 102:422–426